Locally-Activated Chemogenetic pH Probes for Monitoring Protein Exocytosis

Justine Coïs,[1,2] Marie-Laure Niepon[2], Manon Wittwer,[1] Philippe Bun[3], Jean-Maurice Mallet[1], Vincent Vialou[2*] and Blaise Dumat[1*]

[1]Ecole normale supérieure, CNRS, Laboratoire des Biomolécules, France

[2]Sorbonne Université, INSERM, CNRS, Neuroscience Paris Seine, France

[3]Université Paris Cité, Institute of Psychiatry and Neuroscience of Paris (IPNP), INSERM U1266, NeurImag Imaging Core Facility, 75014 Paris, France

*Corresponding authors: vincent.vialou@inserm.fr; blaise.dumat@ens.psl.eu

Abstract

Genetically encoded biosensors based on fluorescent proteins are valuable tools for imaging biological processes with high selectivity. In particular, pH-sensitive fluorescent proteins such as the GFP-derived superecliptic pHluorin (SEP) or pHuji allow tracking of protein trafficking through acidic and neutral compartments. Recently, chemogenetic indicators combining synthetic fluorophores with genetically encoded self-labeling protein tags (SLP-tag) offer a versatile alternative that combines the diversity of chemical probes and indicators with the selectivity of the genetic-encoding. Here, we describe a novel fluorogenic and chemogenetic pH sensor consisting of a cell-permeable molecular pH indicator called **pHluo-Halo-1** whose fluorescence can be locally activated in cells by reaction with the SLP-tag HaloTag ensuring high signal selectivity in wash-free imaging experiments. pHluo-Halo display a good pH sensitivity and a suitable pK_a of 5.9 to monitor biological pH variations. This hybrid chemogenetic pH probe was applied to follow the exocytosis of a CD63-HaloTag fusion proteins enabling the visualization of exosomes released from acidic vesicles into the extracellular media using TIRF microscopy. This chemogenetic platform is expected to be a powerful and versatile tool for elucidating the dynamics and regulatory mechanisms of proteins in living cells.

Key words : pH probes; chemogenetic probes; fluorogenic probes; exocytosis; HaloTag; CD63

Introduction

Exocytosis is a process by which cells are able to release biomolecules (e.g. proteins, neurotransmitters) into the surrounding environment via the fusion of the secretory vesicles to the plasma membrane of cells. It is involved in various critical cellular events such as cell communication, hormone regulation or immune defense.[1] Therefore, precise understanding of exocytosis events is crucial to improve knowledge about physiopathological pathways in various organs including the central nervous system. Over the past decades, significant efforts have been carried out to understand molecular dynamics of exocytosis using fluorescence microscopy techniques.[2–4] In particular, the exocytosis process is associated with varying pH conditions, from typically acidified secretory vesicles (pH 5.5) to neutral compartments and extracellular environment (pH 7.4) and can be visualized by pH-sensitive fluorescent probes such as the superecliptic pHluorin (SEP) derived from the green fluorescent protein.[5] The emission of this pH-sensitive fluorescent protein (FP) is activated when going from acidic to neutral pH with ideal properties for monitoring exocytosis: a pK_a value of 7, cooperative protonation and low background fluorescence in the protonated state.[6] More recently, various red-emitting pH sensitive fluorescent proteins (FPs) such as pHuji[7], pHTomato[8], pHoran4[7] or pHmScarlet[9] with appropriate pK_a values have also been developed. However, protein engineering of pH-sensitive FPs with tuned spectral properties, correct dynamic range and high photostability remains complex. An emerging alternative to FP-based biosensors are chemogenetic (also called hybrid or chemigenetic) biosensors that combine a genetically-encoded self-labeling protein (SLP) tag such as SNAP-tag or HaloTag with an organic fluorophore.[10–12] The latter can be a simple dye for visualizing the target protein or a chemical indicator able to sense its environment. This approach benefits from the unparalleled selectivity of protein genetic encoding and the versatility of fluorescent probes development to enable diverse applications. While protein engineering relies on repeated cycles of evolution to reach the desired properties, organic chemistry benefits from a century-long history of fluorophore development to help the rational design of adequate chemical indicators that can then be coupled to SLP tags. A wide palette of probes or sensors can be combined with a single fusion between a protein of interest and a SLP tag, allowing maximal versatility.[13,14] For instance, a chemogenetic fluorescent pH sensor based on the combination of a pH-sensitive fluorescein derivative with SNAP-tag was recently reported.[15] With a pK_a value of 7.3, it enabled the monitoring of exocytosis and endocytosis and is a credible alternative to SEP. However, in this strategy, the fluorescein-based pH indicator is fluorescent regardless of whether it is linked or not to the target protein, which requires washing steps to remove the excess of probe and avoid off-target signal. In order to match the selectivity of fluorescent protein biosensors, an ideal hybrid sensor should be based on a chemical indicator that is only fluorescent when bound to its target SLP tag. Fluorogenic probes whose emission is activated by the reaction with a SLP-tag have been widely developed for labeling proteins with high selectivity[10,11,16–18] but there are very few examples of hybrid sensors that combine

fluorogenic activation with the ability to detect a biological analyte. For instance, locally-activated sensors for calcium or glutathione based on fluorogenic rhodamines have recently been reported.[19,20] As for pH, Xu and colleagues developed a chemogenetic pH indicator based on 1,8-napthalimide fluorophore (BG-NDM) to monitor intracellular pH using SNAP-tag labeling.[21] Fluorescence of BG-NDM is activated upon both SNAP-tag covalent binding and acidic pH ensuring high accuracy for sensing pH changes in native microenvironment. The Bruchez group developed a hybrid sensor based on the energy transfer (FRET) between malachite green and a pH-sensitive cyanine.[22–24] Selectivity is maintained through the fluorogenic activation of malachite green by genetically-encoded fluorogen-activating proteins (FAPs). However, this dual design exploits the entire visible spectrum making it unsuitable tool for multiplexing imaging and restricting its application to targeting membrane proteins. Therefore, there is still a need for small cell-permeant molecular pH probes that can be activated locally by reaction with an SLP-tag to perform genetically-targeted pH sensing in live cells with high selectivity in wash-free conditions.

In this work, we set out to develop dual-input hybrid pH sensors based on the association of chemically accessible pH-sensitive fluorescent molecular rotors with HaloTag to study protein exocytosis with high selectivity in no-wash imaging conditions (**Figure 1**A). We synthesized a pair of pH-sensitive fluorogenic ligands with close structural similarity to the GFP chromophore, **pHluo-Halo-1** and **pHluo-Halo-2,** that display high fluorescence enhancement upon reaction with HaloTag, good sensitivity to pH and a suitable pK_a to be used in exocytosis imaging. Attempts at red-shifting the emission wavelength by developing analogs of the red Kaede protein chromophore yielded a red-emitting fluorogen but with low pH sensitivity. The most promising probe **pHluo-Halo-1** showed excellent contrast with negligible non-specific signal in confocal imaging of HaloTag-expressing HeLa cells. This is, to the best of our knowledge, the first report of dual-input pH probes locally-activated by reaction with a genetically-encoded protein and we successfully applied the resulting chemogenetic pH sensor to follow the transport and secretion of the exosomal protein CD63 by TIRF microscopy.

Results and discussion

Design of fluorogenic pH probes. To observe exocytosis dynamics, we aimed to develop chemogenetic pH sensors with similar properties as the SuperEcliptic pHluorin (SEP) with a quenched fluorescence in acidic vesicles that instantaneously turns-on upon plasma membrane fusion (**Figure 1**A). The genetically-encoded protein part of our system will be the well-established HaloTag technology that will have to be combined with a fluorogenic and pH sensitive small molecular probe. We have previously shown that small viscosity-sensitive molecular rotors could be used as fluorogenic HaloTag probes and used as a plaftform to build a dual-input calcium sensor.[25–28] We have adapted this approach to design a dual-input pH probe by exploring GFP-based chromophore structures that already possess pH-sensitive properties due to their phenol group and are based on a flexible molecular rotor structure that should also be activated by reaction with HaloTag. However, the pK_a of the isolated GFP chromophore is too high for the biological pH range of exocytosis events.
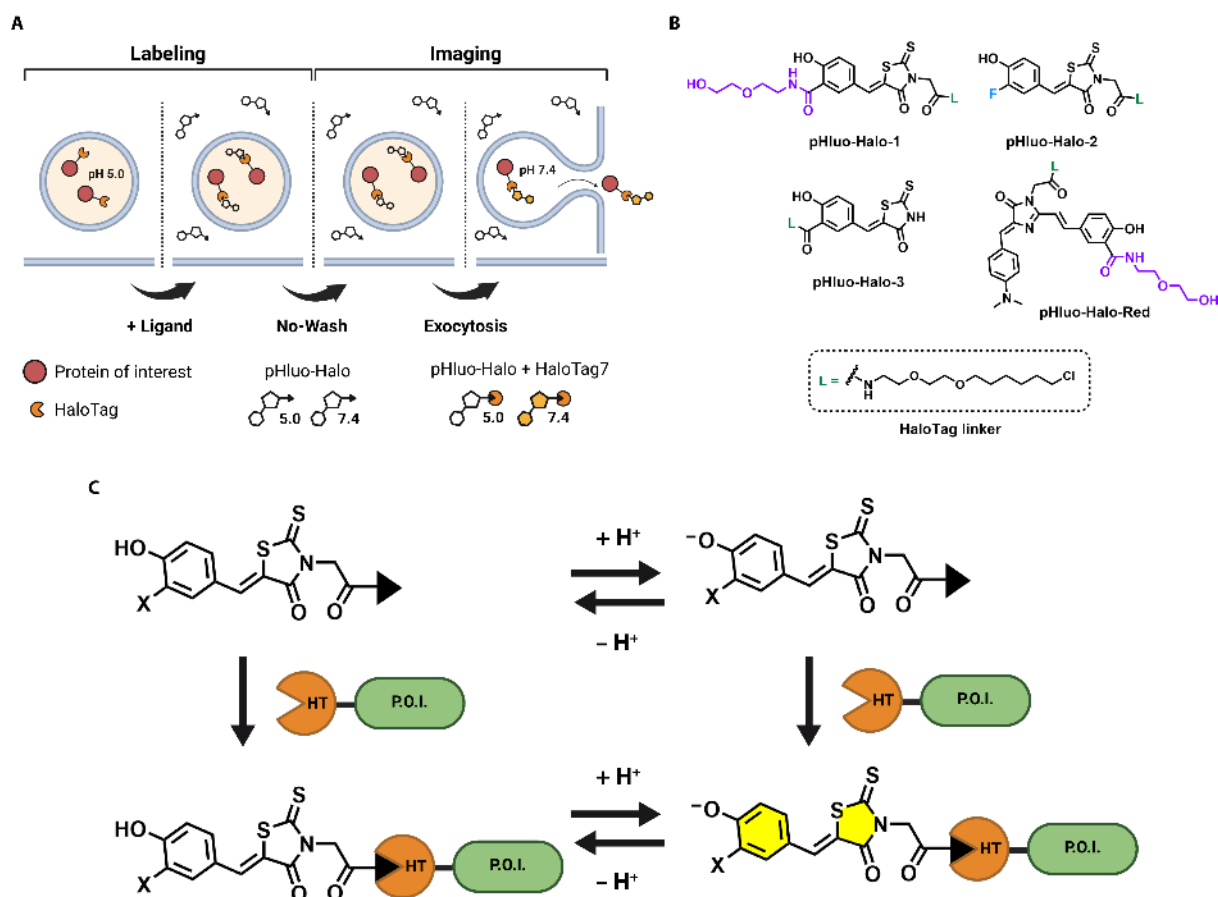
Figure 1 Design and working principles of the pHluo-Halo reporters to monitor protein exocytosis. **A** Schematic description of vesicles expressing HaloTag protein fused to a P.O.I and labeled with a pHluo-Halo ligand to monitor protein exocytosis under no-wash condition. **B** Chemical structures of **pHluo-Halo-1**, **pHluo-Halo-2**, **pHluo-Halo-3** and **pHluo-Halo-Red**. **C** Principle of the dual-input activation of the fluorescence emission of the pHluo-Halo probes.

Therefore, we synthesized HaloTag-targeted GFP analogs with tuned emission properties and pK_a. We first replaced the imidazolone cycle of the GFP chromophore by a rhodanine heterocycle since the resulting structures are easier to synthesize and this electron-withdrawing group proved more efficient in previously reported fluorogenic protein probes (**Figure 1**B).[26,29] To shift the pK_a into a biologically relevant range, we tested two distinct strategies by introducing an amide group (**pHluo-Halo-1**&**3**) or a fluorine atom (**pHluo-Halo-2**) in *ortho* position of the phenol**.** The electron-withdrawing fluorine is a classical strategy to lower the pK_a and obtain chromophores that are deprotonated at neutral pH such as the aptamer fluorogens FHBI and DFHBI.[30] The amide strategy, first reported by Collot *et al.*, assumes that the H-bond between the phenol and the amide is responsible for lowering the pK_a.[31] In **pHluo-Halo-1**, the amide bond was also used to introduce a hydrophilic diethylene glycol chain in order to limit the non-specific activation in cells. Our previous studies on molecular rotor fluorogens indeed showed that the non-specific activation can be mitigated

by lowering their lipophilicity.[27] To allow for specific labeling of recombinant proteins, we introduced a chloroalkane HaloTag linker on the rhodanine group. Since the binding to the

protein may affect the sensing properties of the pH-probes, **pHluo-Halo-3** was synthesized to evaluate an alternative attachment position of the HaloTag linker (**Figure 1**B). To further red-shift the emission wavelength and avoid potential issues with cell autofluorescence, we incorporated the pH-sensitive phenol group using the same amide strategy as **pHluo-Halo-1**&**3**, in a Red Kaede protein chromophore analog to yield **pHluo-Halo-Red** (**Figure 1**B).

The pHluo-Halo probes are based on chemically-accessible structures. The synthesis of the probes **pHluo-Halo-1** to **3** is straightforward and they are easily obtained by a Knoevenagel reaction between a rhodanine group and the corresponding aldehyde (**Scheme S1**). The pHluo-Halo probes are designed to have a pH-sensitive fluorescence emission activated by reaction with HaloTag and these dual-input pH probes should enable pH sensing in the environment of genetically-encoded proteins with high selectivity (**Figure 1**B).

Characterization in 40% glycerol buffers. The pHluo-Halo ligands are push-pull structures with typical molecular rotor features and they display very low fluorescence in water.[32–34] To assess their intrinsic photophysical properties independently of the target protein, the 4 pH-sensitive dyes were first characterized by UV-Vis absorption and fluorescence spectroscopies in buffers containing 40% glycerol to increase the viscosity and activate their fluorescence. The low glycerol content leads to a weak activation of the probes (4-fold enhancement of fluorescence at pH = 7.4) but it is sufficient to characterize them in buffers with controlled pH (**Figure 2**A). For **pHluo-Halo-1**,-**2** and -**3**, the absorption spectra displays two absorption peaks depending on pH corresponding to the protonated and anionic forms of the molecules that are mostly deprotonated at neutral pH (**Figure 2**B and Figure S1), showing that both the fluorine or the amide group successfully lower the pK_a of the phenol. Only the deprotonated form of **pHluo-Halo-1**&-**2** is fluorescent with an emission centered around 560 nm that is red-shifted by 50 nm compared to the GFP chromophore as a result of the stronger electron-withdrawing ability of the rhodanine heterocycle compared to imidazolinone (**Figure 2**A and **Table 1**). The emission of **pHluo-Halo-3** is slightly less red-shifted as has previously been observed for unalkylated rhodanine (λ_{em} = 543 nm).[28] The extended conjugated structure of **pHluo-Halo-Red** based on the Red Kaede protein led to a red fluorescence emission (λ_{em} = 615 nm) even more red-shifted than the parent chromophore (λ_{em} = 582 nm) (**Figure 2**A and **Erreur ! Source du renvoi introuvable.**).[35] An increase of fluorescence intensity with pH was observed for the 4 dyes confirming their pH-sensing ability (**Figure 2**C and Fig. S1). However, the dynamic of **pHluo-Halo-Red** was low, with a fluorescence enhancement ratio of 2 between pH 4.3 and pH 8.3 comparing to a ratio of 12, 55 and 10 for **pHluo-Halo-1**,-**2** and -**3** respectively (**Table 1**). Fluorescence-based pH titrations gave a pK_a of 6.0 for both **pHluo-Halo-1**&-**3** and a pK_a of 6.6 for **pHluo-Halo-2** (**Figure 2**D, **Table 1** and **Figure S1**).The measured pK_a values are slightly lower than that of SEP but are still relevant for the biological pH range involved during exocytosis. For **pHluo-Halo-Red,** a pK_a value of 7.6 was measured (**Table 1** and **Figure S1**). Despites the its red-shifted emission, the pH sensitivity of pHluo-Halo-Red is not sufficient and it was not studied further.
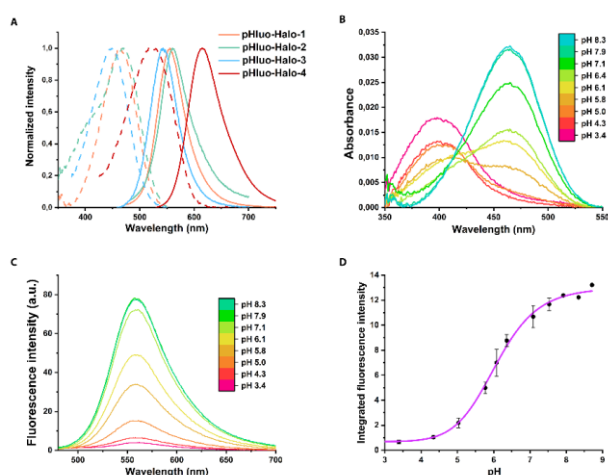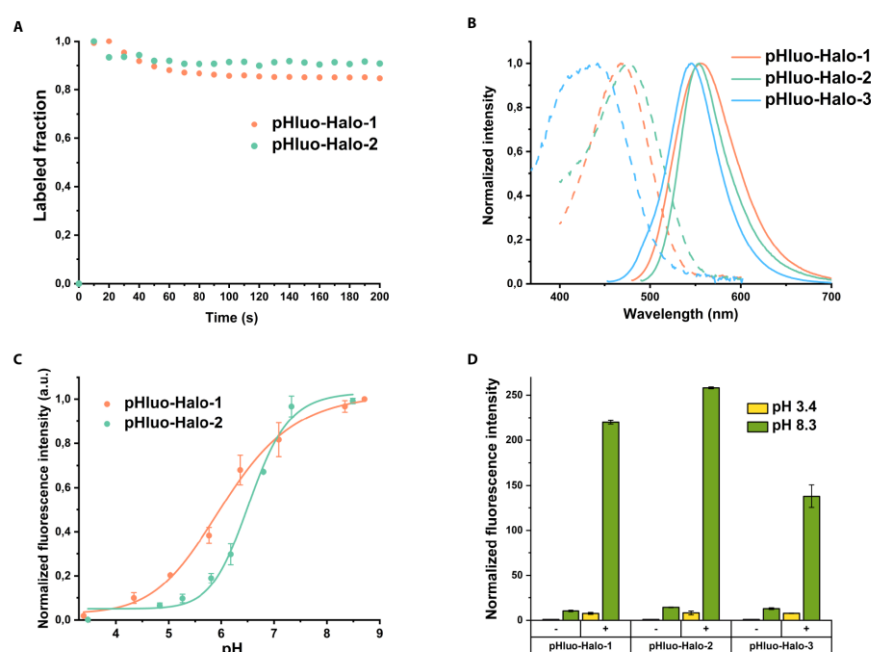
Figure 2 Characterization of chemogenetic fluorogenic pH probes in tris buffers with 40 %w/v of glycerol. **A** Absorbance (dashed lines) and fluorescence emission (full lines) spectrum of pHluo-Halo probes. **B** UV-vis and **C** fluorescence pH titration of **pHluo-Halo-1** in TRIS buffers with 40 %w/v glycerol **D** Fluorimetric pH titration curve of **pHluo-Halo-1** (pK_a = 6.0). Mean + SD of two independent experiments.

Given that the **pHluo-Halo-1-3** probes exhibit two distinct excitation spectra depending on pH, they can be used as well as excitation-ratiometric pH probes to perform quantitative pH measurement in cells. This is not necessary for the envisioned application in this work (exocytosis imaging) but it could be useful for other application and the radiometric response and calibrating curves were measured (Figure S2).[5]

Table 1 Photophysical properties of pHluo-Halo probes in glycerol and in presence of HaloTag protein in PBS (pH = XX?). λ_{abs} and λ_{em} maximum absorption and emission wavelength, ε: molar absorptivity coefficient, Φ_F: fluorescence quantum yield, $\varepsilon.\Phi_F$: brightness, F(HaloTag)/F(PBS) : fluorescence enhancement factor where F(HaloTag) and F(PBS) are the integrated fluorescence intensities in HaloTag and in PBS respectively. F(pH 8.3)/F(pH 4.3) : fluorescence enhancement factor where F(pH 8.3) and F(pH 4.3) are the integrated fluorescence intensities of pHluo-Halo probes bound to HaloTag at pH 8.3 and pH 4.3 respectively. [a] Measurement conditions: 1 µM dye with 1.5 eq. of HaloTag in pH 8.3 TRIS (0.05 M) buffer containing 100 mM NaCl, [b] Average of duplicate experiments.

Molecule	Solvent /Target	λ_{abs} (nm)[a]	ε (M^{-1}.cm^{-1})	λ_{em} (nm)[a]	Φ_F	$\varepsilon.\Phi_F$	$F_{HaloTag}/F_{PBS}$[b]	$F_{pH8.3}/F_{pH4.3}$[b]	pK_a[b]
pHluo-Halo-1	Glycerol (40%)	465	-	556	-	-	-	12	6.0
	HaloTag	470	42 500	553	0.04	1900	21	29	5.9
pHluo-Halo-2	Glycerol (40%)	468	-	560	-	-	-	55	6.6
	HaloTag	478	28 400	553	0.01	340	18	31	6.5
pHluo-Halo-3	Glycerol (40%)	449	-	543	-	-	-	10	6.2
	HaloTag	442	18 000	546	0.01	220	8	18	6.4
pHluo-Halo-Red	Glycerol (40%)	524	-	615	-	-	-	2	7.6

Characterization in HaloTag. The characterization in glycerol allowed us to determine the intrinsic pH-dependence of the photophysical properties of the pHluo-Halo molecular probes. These properties were next evaluated after reaction with HaloTag to study the influence of the protein environment on the fluorescence emission and on the pH sensing ability. We observed in our previous studies with molecular rotors that the rate constants of the reaction with HaloTag were much slower that the one reported for Halo-TMR (10^7 $M^{-1}.s^{-1}$).[26,27] In the case of the pHluo-Halo probes, the reaction is quasi-instantaneous and too fast to measure the reaction rate constant using fluorescence spectroscopy. It is associated with a strong increase of fluorescence with similar wavelengths as observed in 40% glycerol buffer (**Figure 3A&B**).


Figure 3 Reaction of the pHluo-Halo probes with HaloTag and characterization of the resulting chemogenetic pH sensors. **A** Reaction kinetics of **pHluo-Halo-1** (Orange) and pHluo-Halo2 (green) with HaloTag. Conditions: [dye] = 100 nM, [HT] = 2 μM, T = 298 K. **B** Normalized absorption and fluorescence intensity of **pHluo-Halo-1**, **pHluo-Halo-2** and **pHluo-Halo-3** (1 μM) in HaloTag (1.5 eq.) at pH 7.4. **C** pH titration curve of **pHluo-Halo-1**&**2** conjugated to HaloTag. Mean + SD of two independent experiments **D** Dual-input activation of fluorogenic pH probes. Fluorescence intensity normalized to integrated fluorescence of pHluo-Halo probe in PBS at pH 3.4 : the four states are represented (-) HaloTag at pH 3.4 (yellow); (+) HaloTag at pH 3.4 (yellow); (-) HaloTag at pH 8.3 (green) and (+) HaloTag at pH 8. (green) for **pHluo-Halo-1-3**.

The probes display comparable pH sensitivity in HaloTag than in glycerol, with similar pK_a values, although slight differences in the dynamic range were observed: **pHluo-Halo-1&2** exhibit a ratio F(pH = 8.3)/F(pH = 3.4) of 29 and 31 respectively while **pHluo-Halo-3** displays

poorer pH sensitivity with a ratio of 18 (**Erreur ! Source du renvoi introuvable.**). The pH-sensitive **pHluo-Halo1**&-**2** probes exhibit the desired dual-input fluorescence properties with a good pH sensitivity and a strong activation of the fluorescence upon reaction with HaloTag with up to a 21-fold increase for **pHluo-Halo-1** (Figure 3D, Table 1). However, due to its moderate fluorescence activation (8-fold increase) and pH sensitivity, **pHluo-Halo-3** was not further studied.

Evaluation of chemogenetic pHluo-Halo indicators in live cells. We next examined the properties of the selected dyes **pHluo-Halo-1** and **pHluo-Halo-2** in fluorescence imaging of live HeLa cells either wild-type or expressing a nuclear HaloTag protein to assess their selectivity and contrast under wash-free conditions. In non-transfected HeLa cells incubated with 0.5 µM of **pHluo-Halo-1** and -**2** without any washing steps (Fig. S3), **pHluo-Halo-1** gave a negligible fluorescence signal, while **pHluo-Halo-2** exhibited a detectable non-specific signal. This is consistent with our hypothesis that the non-specific activation is linked to the lipophily of the probes. Imaging of HeLa cells expressing a HaloTag-NLS protein after incubation of probes with the same protocol revealed efficient HaloTag labeling demonstrating that these 2 dyes are cell permeable and react selectively with HaloTag in cells (**Erreur ! Source du renvoi introuvable.**A). The comparison of the cytosolic background fluorescence intensity in non-expressing cells *versus* the nuclear signal of expressing cells revealed that **pHluo-Halo-1** exhibits excellent signal-to-background ratio (F_{nuc}/F_{cyt} = 40) contrary to **pHluo-Halo-2** (F_{nuc}/F_{cyt} = 5,2), which is consistent with the relative non specific signals observed in wild-type HeLa cells (**Erreur ! Source du renvoi introuvable.**B).
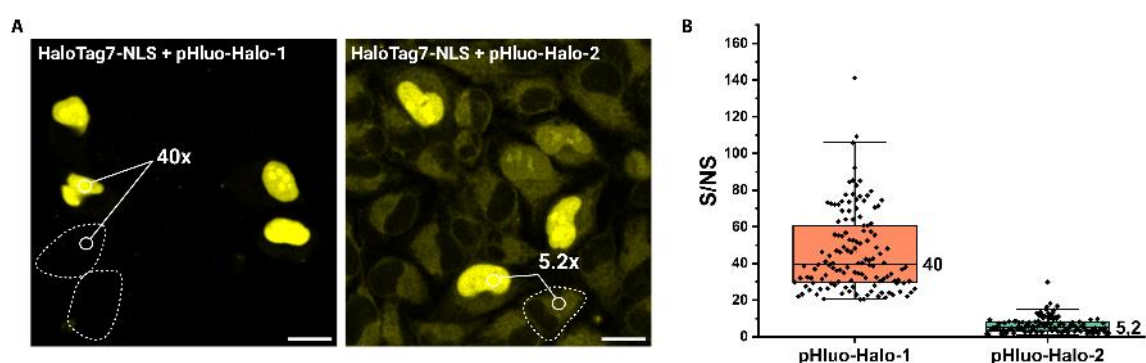
Figure 4 Selectivity of the pHluo-Halo probes in live HeLa cells. **A** confocal microscopy images of HaloTag-NLS-expressing and non-expressing HeLa cells. Cells were incubated with 0.5 µM **pHluo-Halo-1** (left) and **pHluo-Halo-2** (right) for 10 min and imaged under no-washed conditions. The signal is measured in the nuclei of transfected cells, while the background is measured in the cytoplasm of non-

transfected cells. Turn-on numbers represent average of n = 130 cells. Scale bar = 20 µm. **B** Contrast of **pHluo-Halo-1** and **pHluo-Halo-2** measured in HeLa cells expressing HaloTag-NLS of n = 130 cells.

Detection of single exocytosis events in HeLa cells. To test the efficiency and capability of our novel pH-sensitive dual-input chemogenetic system for monitoring exocytosis, we used the well-characterized tetraspanin protein CD63 as a model (**Figure 5A**).[36,37] CD63 is a transmembrane protein located in exosomes, which are small endosome-derived extracellular vesicles found in multivesicular bodies (MVB). These vesicles play a crucial role in cell-cell communication,[37] and are released when MVBs fuse with the plasma membrane (PM). Building on the existing CD63-SEP construct, we designed a CD63-HaloTag construct and first confirmed its expression in HeLa cells by western-blotting (Fig. S4). Subsequently, we tracked the exocytosis of CD63 in HeLa cells using Total Internal Reflection Fluorescence (TIRF) microscopy, a technique commonly used to monitor alterations in the fluorescence intensity of a pH-sensitive FP at the PM of cells. Thus, it is ideally suited to detect single-vesicle exocytosis events.[5,6,38–40] For data analysis, we used the recently developed ExoJ plugin for automatic and accurate detection of single exocytic events.[41] Time-lapse live imaging of 2 min enabled the detection of multiple fusion events scattered across the PM under basal condition. These events were characterized by as an abrupt brightening followed by spreading of the fluorescence signal (**Figure 5B**). We focused on MVB-PM fusion events that display an intensity profile similar to **Figure 5B**. Although a proportion of exosomes remain attached to the cell surface,[42] they were not included in our analysis. To validate the specificity of our **pHluo-Halo-1** labeling through CD63-tagged exosomes, we performed simultaneous dual-color TIRF microscopy using co-transfected HeLa cells expressing both CD63-pHuji and CD63-HaloTag constructs (**Figure 5C**).[39] We observed colocalization of vesicles between CD63-pHuji and CD63-HaloTag labeled with **pHluo-Halo-1** with similar fluorescence dynamic of exocytosis events (**Figure 5C**). We calculated a Pearson's coefficient of 90% for the colocalization between exosomes labeled with CD63-pHuji and exosomes labeled with CD63-HaloTag conjugated to **pHluo-Halo-1** indicating significant overlap of fusion events in HeLa cells (Figure S5). These results confirmed the specificity of the CD63 labeling using our locally activated chemogenetic pH probe in living-cells. To further evaluate our chemogenetic pH probes, we decided to stimulate HeLa cells with histamine (**Figure 5D**). Histamine has been previously shown to stimulates MVB-PM fusion activity and the secretion of CD63.[37,39] Consequently, upon addition of 100 µM histamine, the rate of fusion events between MVB and the PM

immediately increased compared to basal fusion activity. The higher number of detected events could be attributed to increased fluorescence intensity (**Figure 5D**). However, the exocytic events detected between basal conditions and stimulated cells exhibited comparable normalized peak intensity ($\Delta F/F_0$) (**Figure 5E**), indicating an increase in the exocytosis of MVB. To assess the accuracy of the identification of fusion events using our chemogenetic pH-sensitive probe, we compared intrinsic parameters such as apparent vesicles size and fusion duration with values obtained with the well-established SEP biosensor (**Figure 5F&G**). The quantitative estimation of apparent sizes of events reported by CD63-SEP and CD63-HaloTag labeled with **pHluo-Halo-1** were similar (around 150 nm) with each other and consistent with previous qualitative analysis at supra-optical electron microscopy resolution using a dynamic correlative light electron microscopy approach (**Figure 5F**).[37] Likewise, the mean lifetime decay (τ, ns) of both constructs with regards to fusion duration, were of similar duration regardless of histamine stimulation (**Figure 5G**).

Therefore, our chemogenetic pH-sensitive scaffold is able to detect exocytosis events with similar biological parameters as SEP in live HeLa cells. The excellent contrast and pH sensitivity of the pHluo-Halo ligands associated with HaloTag make this platform a powerful and versatile alternative to FP-based pH probes.
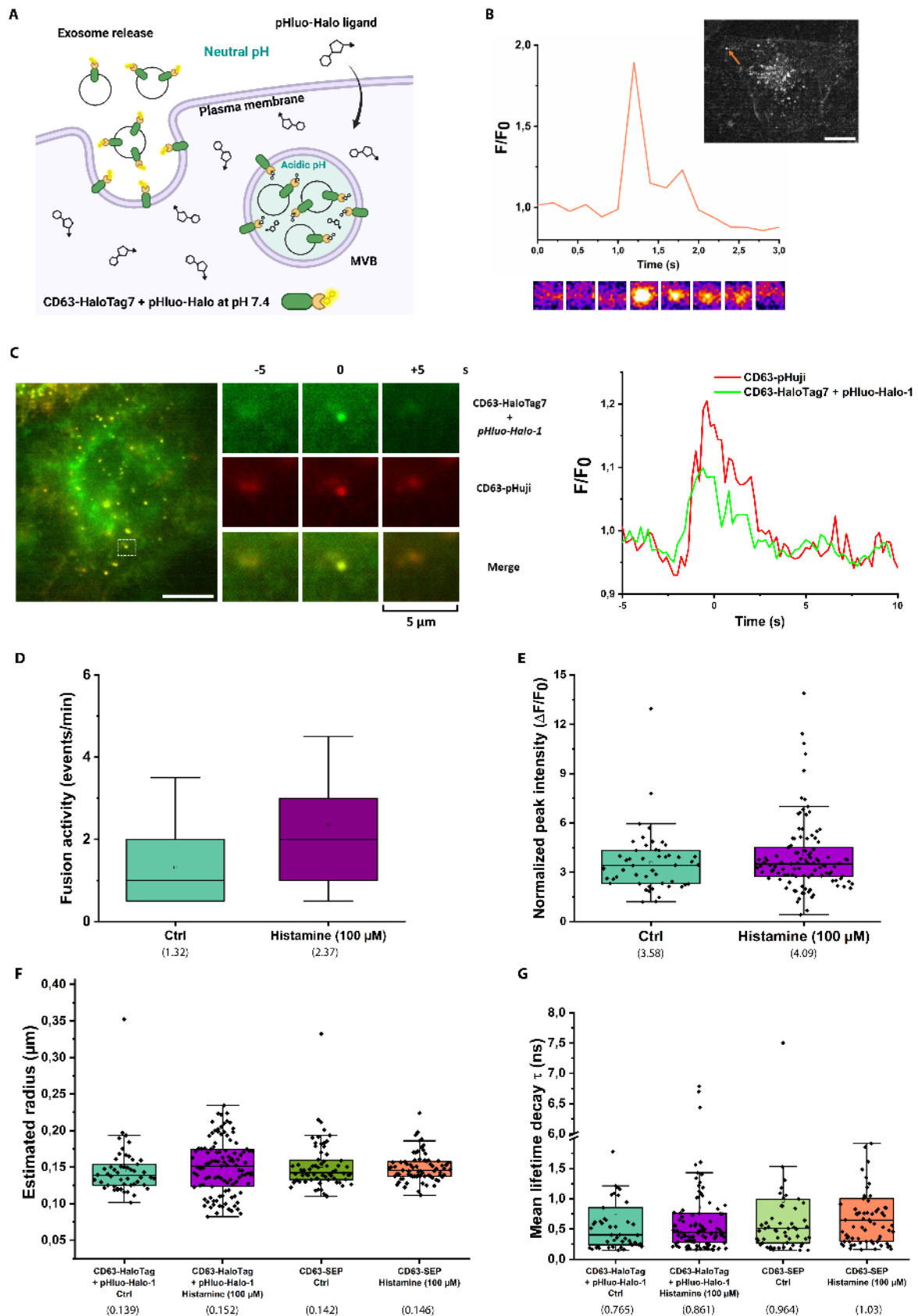
Figure 5 Detection of single CD63 exocytosis in HeLa cells. **A** Experimental scheme: prior to imaging, CD63-HaloTag transfected HeLa cells were incubated with cell-permeable **pHluo-Halo-1** ligand to specifically label CD63-HaloTag fusion proteins. **B** TIRF microscopy images of HeLa cell expressing

CD63-HaloTag labeled with **pHluo-Halo-1** undergoing fusion. Image of the whole cell with a fusion event indicated with orange arrow (top); Normalized intensity traces for a selected fusion event (bottom) ; Time-lapse of the marked exocytotic event (middle, 5 µm); **C** Left, merged stills of dual-color TIRF imaging with CD63-SEP and CD63-HaloTag labeled with **pHluo-Halo-1** (top) at the moment of MVB-PM fusion (in the white dashed square). Scale bar, 10 µm. Enlarged stills of the MVB-PM fusion event 10 s before fusion, at the moment of fusion, and 10 s after fusion (middle). Normalized intensity traces for the marked fusion event labeled with CD63-HaloTag + **pHluo-Halo-1** (Green) and CD63-pHuji (Red). **D** Comparison of fusion activity of HeLa cells stimulated with histamine (100 µM). $n \geq 8$ per condition. **E** Comparison of normalized peak intensity ($\Delta F/F_0$) of fusion events from CD63-HaloTag labeled with **pHluo-Halo-1** in basal condition (ctrl) and after histamine stimulation (100 µM). **F** Apparent size of single vesicles population labeled with CD63-SEP and CD63-HaloTag + **pHluo-Halo-1** in basal condition and after histamine stimulation (100 µM). **G** Event duration τ (ns) of fusion events from CD63-HaloTag labeled with **pHluo-Halo-1** in basal condition (ctrl) and after histamine stimulation (100 µM).

Conclusion & perspectives

We developed of a locally-activated chemogenetic pH sensor that enables imaging protein exocytosis in live cells with high selectivity. Unlike other existing organic pH indicators such as rhodamine, cyanine or fluorescein dyes,[15,43–45] our chemogenetic sensor benefits from the targeting selectivity of the genetically encoded protein HaloTag combined with tunable, chemically accessible pH-sensitive ligands. This system offers excellent contrast, low background and very fast incubation time, making it a powerful tool for performing fluorescence imaging under no-wash conditions. This is, to the best of our knowledge the first genetically encoded dual-input pH probes with a locally-activated fluorescence upon HaloTag reaction. It was applied to monitor the exocytosis of the CD63 protein exocytosis and exhibited excellent event detection with similar intrinsic biological properties as those observed using super ecliptic pHluorin (SEP). Recent examples show that HaloTag engineering can improve the interaction and fluorogenic activation of fluorogenic probes.[28,46] In the future, the combination of protein and molecular engineering could help further improving such chemogenetic sensors.

Acknowledgments

References

1.   Anantharam, A. & Knight, J. Exocytosis: From molecules to cells. *Exocytosis From Mol. to Cells* 1–129 (2022) doi:10.1088/978-0-7503-3771-7.

2.   Li, W. hong. Probes for monitoring regulated exocytosis. *Cell Calcium* **64**, 65–71 (2017).

3.   Li, W. H. & Li, D. Fluorescent probes for monitoring regulated secretion. *Curr. Opin. Chem. Biol.* **17**, 672–681 (2013).

4.   Amatore, C., Arbault, S., Guille, M. & Lemaître, F. Electrochemical monitoring of single cell secretion: Vesicular exocytosis and oxidative stress. *Chem. Rev.* **108**, 2585–2621 (2008).

5.   Gero Miesenböck, Dino A. De Angelis & James E. Rothman. Visualizing secretion and synaptic transmission with pH-sensitive green fluorescent proteins. *Nature* **394**, 192–195 (1998).

6.   Sankaranarayanan, S., De Angelis, D., Rothman, J. E. & Ryan, T. A. The use of pHluorins for optical measurements of presynaptic activity. *Biophys. J.* **79**, 2199–2208 (2000).

7.   Shen, Y., Rosendale, M., Campbell, R. E. & Perrais, D. pHuji, a pH-sensitive red fluorescent protein for imaging of exo- and endocytosis. *J. Cell Biol.* **207**, 419–432 (2014).

8.   Li, Y. & Tsien, R. W. PHTomato, a red, genetically encoded indicator that enables multiplex interrogation of synaptic activity. *Nat. Neurosci.* **15**, 1047–1053 (2012).

9.   Liu, A. *et al.* pHmScarlet is a pH-sensitive red fluorescent protein to monitor exocytosis docking and fusion steps. *Nat. Commun.* **12**, (2021).

10.   Los, G. V. *et al.* HaloTag: A Novel Protein Labeling Technology for Cell Imaging and Protein Analysis. *ACS Chem. Biol.* **3**, 373–382 (2008).

11.   Hoelzel, C. A. & Zhang, X. Visualizing and Manipulating Biological Processes by Using HaloTag and SNAP-Tag Technologies. *ChemBioChem* vol. 21 1935–1946 at https://doi.org/10.1002/cbic.202000037 (2020).

12.   Sun, X. *et al.* Development of SNAP-tag fluorogenic probes for wash-free fluorescence imaging. *ChemBioChem* **12**, 2217–2226 (2011).

13.   Cook, A., Walterspiel, F. & Deo, C. HaloTag-Based Reporters for Fluorescence Imaging and Biosensing. *ChemBioChem* **24**, e202300022 (2023).

14.   Broch, F., Gautier, A., Broch, F. & Gautier, A. Illuminating Cellular Biochemistry: Fluorogenic Chemogenetic Biosensors for Biological Imaging. *Chempluschem* **85**, 1487–1497 (2020).

15.   Martineau, M. *et al.* Semisynthetic fluorescent pH sensors for imaging exocytosis and endocytosis. *Nat. Commun.* **8**, 1412 (2017).

16.   Keppler, A. *et al.* A general method for the covalent labeling of fusion proteins with small molecules in vivo. *Nat. Biotechnol.* **21**, 86–9 (2003).

17.   Gautier, A. *et al.* An Engineered Protein Tag for Multiprotein Labeling in Living Cells. *Chem. Biol.* **15**, 128–136 (2008).

18.   Hori, Y. *et al.* Development of fluorogenic probes for quick No-Wash live-cell imaging of intracellular proteins. *J. Am. Chem. Soc.* **135**, 12360–12365 (2013).

19.   Mertes, N. *et al.* Fluorescent and Bioluminescent Calcium Indicators with Tuneable Colors and Affinities. *J. Am. Chem. Soc.* **144**, 6928–6935 (2022).

20.   Emmert, S., Quargnali, G., Thallmair, S. & Rivera-Fuentes, P. A locally activatable sensor for robust quantification of organellar glutathione. *Nat. Chem.* **15**, 1415–1421 (2023).

21.   Xu, N. *et al.* Protein proximity ligation probe with wide sensing range resolving dynamics of subcellular ph by super-resolution imaging. *Sensors Actuators B Chem.* **398**, 134744 (2024).

22.   Bruchez, M. P. Dark dyes-bright complexes: Fluorogenic protein labeling. *Curr. Opin. Chem. Biol.* **27**, 18–23 (2015).

23.   Grover, A. *et al.* Genetically encoded pH sensor for tracking surface proteins through endocytosis. *Angew. Chemie - Int. Ed.* **51**, 4838–4842 (2012).

24.   Perkins, L. A. *et al.* Genetically Targeted Ratiometric and Activated pH Indicator Complexes (TRApHIC) for Receptor Trafficking. *Biochemistry* **57**, 861–871 (2018).

25.   Bachollet, S. P. J. T., Pietrancosta, N., Mallet, J. & Dumat, B. Fluorogenic and genetic targeting of a red-emitting molecular calcium indicator. *Chem. Commun.* **58**, 6594–6597 (2022).

26.   Bachollet, S. P. J. T., Addi, C., Pietrancosta, N., Mallet, J.-M. & Dumat, B. Fluorogenic Protein Probes with Red and Near-Infrared Emission for Genetically Targeted Imaging**. *Chem. – A Eur. J.* **26**, 14467–14473 (2020).

27.   Bachollet, S. P. J. T. *et al.* An expanded palette of fluorogenic HaloTag probes with enhanced contrast for targeted cellular imaging. *Org. Biomol. Chem.* **20**, 3619–3628 (2022).

28.   Coïs, J. *et al.* Design of Bright Chemogenetic Reporters Based on the Combined Engineering of Fluorogenic Molecular Rotors and of the HaloTag Protein. *Chem. – A Eur. J.* (2024) doi:10.1002/chem.202400641.

29.   Plamont, M.-A. *et al.* Small fluorescence-activating and absorption-shifting tag for tunable protein imaging in vivo. *Proc. Natl. Acad. Sci.* **113**, 497–502 (2016).

30.   Santra, K., Geraskin, I., Nilsen-Hamilton, M., Kraus, G. A. & Petrich, J. W. Characterization of the Photophysical Behavior of DFHBI Derivatives: Fluorogenic Molecules that Illuminate the Spinach RNA Aptamer. *J. Phys. Chem. B* **123**, 2536–2545 (2019).

31.   Despras, G. *et al.* H-Rubies, a new family of red emitting fluorescent pH sensors for living cells. *Chem. Sci.* **6**, 5928–5937 (2015).

32.   Haidekker, M. A. & Theodorakis, E. A. Molecular rotors - Fluorescent biosensors for viscosity and flow. *Org. Biomol. Chem.* **5**, 1669–1678 (2007).

33. Paez-Perez, M. & Kuimova, M. K. Molecular Rotors: Fluorescent Sensors for Microviscosity and Conformation of Biomolecules. *Angew. Chemie Int. Ed.* **63**, (2024).

34. Lee, S. C. *et al.* Fluorescent Molecular Rotors for Viscosity Sensors. *Chem. - A Eur. J.* **24**, 13706–13718 (2018).

35. Miyawaki, A., Shcherbakova, D. M. & Verkhusha, V. V. Red fluorescent proteins: Chromophore formation and cellular applications. *Curr. Opin. Struct. Biol.* **22**, 679–688 (2012).

36. Sung, B. H. *et al.* A live cell reporter of exosome secretion and uptake reveals pathfinding behavior of migrating cells. *Nat. Commun.* **11**, 1–15 (2020).

37. Verweij, F. J. *et al.* Quantifying exosome secretion from single cells reveals a modulatory role for GPCR signaling. *J. Cell Biol.* **217**, 1129–1142 (2018).

38. Burchfield, J. G., Lopez, J. A., Mele, K., Vallotton, P. & Hughes, W. E. Exocytotic vesicle behaviour assessed by total internal reflection fluorescence microscopy. *Traffic* **11**, 429–439 (2010).

39. Bebelman, M. P. *et al.* Real-time imaging of multivesicular body–plasma membrane fusion to quantify exosome release from single cells. *Nat. Protoc.* **15**, 102–121 (2020).

40. Schmoranzer, J., Goulian, M., Axelrod, D. & Simon, S. M. Imaging Constitutive Exocytosis with Total Internal Reflection Fluorescence Microscopy. in *Journal of Cell Biology* vol. 149 23–22 (2000).

41. Liu, J., Verweij, F. J., Niel, G. Van, Danglot, L. & Bun, P. ExoJ: an ImageJ2/Fiji plugin for automated spatiotemporal detection of exocytosis. *bioRxiv* 2022.09.05.506585 (2022).

42. Edgar, J. R., Manna, P. T., Nishimura, S., Banting, G. & Robinson, M. S. Tetherin is an exosomal tether. *Elife* **5**, 1–19 (2016).

43. Georgiev, N. I., Krasteva, P. V. & Bojinov, V. B. A ratiometric 4-amido-1,8-naphthalimide fluorescent probe based on excimer-monomer emission for determination of pH and water content in organic solvents. *J. Lumin.* **212**, 271–278 (2019).

44. Yuan, C., Li, J., Xi, H. & Li, Y. A sensitive pyridine-containing turn-off fluorescent probe for pH detection. *Mater. Lett.* **236**, 9–12 (2019).

45. Myochin, T. *et al.* Rational design of ratiometric near-infrared fluorescent pH probes with various pKa values, based on aminocyanine. *J. Am. Chem. Soc.* **133**, 3401–3409 (2011).

46. Miró-Vinyals, C., Stein, A., Fischer, S., Ward, T. R. & Deliz Liang, A. HaloTag Engineering for Enhanced Fluorogenicity and Kinetics with a Styrylpyridium Dye. *ChemBioChem* **22**, 3398–3401 (2021).